UNIVERSITY OF CALIFORNIA,
IRVINE

Implications of Organic-Sulfate Interactions in Post-Volcanic Aerosol Chemistry and Climate Relevant Radiative Forcing

RESEARCH THESIS

Submitted in partial satisfaction of the requirements for graduation
with honors research distinction in Chemistry in the College
of Physical Sciences of the University of California, Irvine

by

Noam Levi

Thesis Committee:
Professor Sergey Nizkorodov
Professor A.J. Shaka

2025

Table of contents

1. INTRODUCTION TO AEROSOLS.

Aerosols are liquid or gas particles suspended in a gas, with atmospheric aerosol particles typically ranging from a few nanometers to tens of micrometers in diameter. These particles remain suspended long enough to be transported from local to intercontinental scales, depending on their size, density, and meteorological conditions (Seinfeld & Pandis 2016). Aerosols influence climate by scattering and absorbing radiation, modifying cloud microphysics, and altering atmospheric chemistry. They also affect air quality and human health by penetrating into the respiratory tract (Delmotte et al., 2021; Lelieveld et al., 2015).

In the atmospheric sciences community, the term "aerosols" includes the suspending gas phase (N_2, O_2, Ar, CO_2, etc.) and macroscopic hydrometeors such as raindrops, hail, and snowflakes (Pöschl 2005). However, the term "aerosol particles" was coined when referring to particulate matter in aerosol, excluding the suspending gas (Laskin et al., 2015). For simplicity, the term "aerosol" is often used to apply to aerosol particles without the suspending gas, and this is the convention used in this thesis.

Aerosols are introduced into the atmosphere through both primary emissions and secondary formation, through the direct release of particles or gas-to-particle conversion chemistry at higher altitudes, respectively. Their sources include natural processes such as desert dust uplift, sea spray, volcanic eruptions, and wildfires, as well as anthropogenic activities including fossil fuel combustion, industrial emissions, and biomass burning for energy or land clearing (Andreae & Rosenfeld 2008; Boucher et al., 2013).

1.1 Aerosol Classes.

Aerosol classifications are essential to understanding our atmosphere, as they can differ by origin, formation mechanism, size or composition. Because their chemical composition most directly determines their reactivity, optical properties, and aging pathways, this section focuses on composition-based classes.

1.1.1 Primary and Secondary Aerosol Classifications. Aerosols can be divided into two classes: *primary* and *secondary*. Primary aerosols are emitted directly into the atmosphere as particulate matter, through either natural or anthropogenic processes. Secondary aerosols are formed from gas-phase species in the atmosphere during the condensation of *aerosol precursors* (Boucher 2015). These gas-phase particles can also undergo chemical transformation prior to condensation (Laskin et al., 2015), leading to a wider variety of secondary aerosols in the atmosphere; hence, investigating secondary aerosol formation is of highly interest in the atmospheric community.

Primary and secondary aerosols encompass a wide variety of particulate matter, thus further classification is required to better understand aerosol optical properties and chemical behavior. Aerosols can be classified by source of emission giving rise to the following classes: mineral dust, sea-spray, combustion, and biological. Aerosols are further classified based on predominant composition as either organic, inorganic or mixed.

1.1.2 Mineral Dust Aerosols. Mineral dust aerosols are inorganic aerosol particulates lifted from land surfaces, particularly in arid and semi-arid regions with little vegetation and low humidity, such as deserts. Winds suspend mineral dust particles into the atmosphere, where they can be transported over long distances (Boucher 2015). These particles are primarily made up of silicates, carbonates, and trace metals, capable of scattering and absorbing incoming radiation. In addition to their radiative effects, mineral dust can interact with anthropogenic pollution, altering the particles' chemical reactivity and optical properties through heterogeneous chemistry (Laskin et al., 2015).

1.1.3 Marine/Sea Spray Aerosols. Marine aerosols are generated by wind, wave breaking and bubble bursting at the ocean surface, ejecting droplets into the atmosphere. As water evaporates, salt concentration increases, leaving behind hydrated sodium chloride, magnesium, calcium, potassium salts, and organic matter particulates (O'Dowd & De Leeuw 2007). However, impurities such as biological material may persist in these droplets, which is why this class of aerosols is more broadly referred to as sea spray aerosols (Boucher 2015). Biological material such as protein and polysaccharides in these particulates makes for an important source of cloud condensation nuclei (CCN), contributing to cooling effects in the atmosphere due to their reflective properties (Després et al., 2012).

1.1.4 Biomass Burning Organic Aerosols. The focus of this thesis is centered around Biomass Burning Organic Aerosols (BBOA), emitted during burning of biological materials, predominantly trees, bushes, and grasses. More broadly, this includes burning of any vegetation-derived biomass, such as wood, animal dung, or peat while excluding fossil fuel smoke aerosols such as coal, gas or oil (Boucher 2015). BBOA fall into a larger class of carbonaceous aerosols, all of which release 3 distinct types of carbon based particulates.

1.1.5 Carbonaceous Aerosols. Carbonaceous aerosols represent one of the most chemically complex and climatically significant categories. This aerosol class consists of particles released through burning events, including smoke aerosols, polluted aerosols, and fossil fuel combustion aerosols. These aerosols are generated and suspended into the atmosphere during burning events such as fires, industrial emissions, volcanic eruptions, and the burning of fossil fuels (Boucher, 2015). They can be broadly divided into black carbon (BC) and organic carbon (OC), based on the thermal characteristics of the compounds from which the particles are made (Laskin et al., 2015).

BC is produced through incomplete combustion, and often used synonymously with elemental carbon (soot) (Laskin et al., 2015). BC has a high carbon content, resulting in strongly light-absorbing visibly black compounds. BC absorbs broadly across the visible spectrum, contributing to atmospheric warming (Bond et al., 2013).

OC encompasses a wide range of primary and secondary organic compounds with either light-absorbing or scattering properties. Organic aerosols are complex mixtures of thousands of compounds containing C, H, O, and sometimes N, S, or Cl. OC can be directly emitted as primary organic aerosol (POA) during burning events or formed in the atmosphere as secondary organic aerosol (SOA) through the oxidation of VOCs (Laskin et al., 2015).

Brown carbon (BrC) is a type of OC of particular importance, as it absorbs solar radiation in the near-UV and visible region, but with a wavelength dependence distinct from BC. BrC originates from both direct emissions, such as biomass burning, and secondary processes, including aqueous-phase reactions of amino acids and other organics (Laskin et al., 2015). BrC is especially relevant to this thesis, as its optical properties and atmospheric lifetime are strongly influenced by chemical aging.

1.1.6 Biological Aerosols. Bioaerosols include particles of biological origin such as pollen, spores, bacteria, viruses, amino acids, and fragments of plant or animal material. They are released naturally but often interact with other aerosol types. These aerosols play an important role especially as ice nuclei (Després et al., 2012); thereby linking biological activity directly to climate processes.

1.1.7 Inorganic Aerosols. Inorganic aerosols are composed of ions such as nitrate, ammonium, chloride and sulfate (Seinfeld & Pandis 2016). Nitrate ions are produced from nitrogen oxides released by vehicles, power plants, lightning, and biomass burning (Xin et al., 2023). Ammonia, largely from agricultural activities and livestock, neutralizes acidic species to form ammonium salts such as ammonium sulfate and ammonium nitrate (Squizzato et al., 2012). Chloride is mainly derived from sea

spray, though it can also be generated by biomass burning and coal combustion (Boucher 2015). Sulfates form largely from the oxidation of sulfur dioxide emitted from fossil fuel combustion, industrial activities, volcanic eruptions, and marine dimethyl sulfide; and are among the most studied due to their strong hygroscopicity and their indirect role in secondary organic aerosol formation via acid catalysis of organic precursors (Kremser et al., 2016). Ammonium sulfate and sulfuric acid droplets are especially important as reaction media for organic compounds, facilitating aqueous-phase chemistry that contributes to secondary organic aerosol (SOA) and BrC formation (Laskin et al., 2015).

1.2 Aerosol Formation.

Atmospheric aerosol formation can be categorized into two main pathways: (i) primary emission of particles and (ii) secondary formation via gas-to-particle conversion. Following particle generation or formation, growth by heterogeneous and interfacial chemistry determines aerosol impact on human health, visibility, radiation, and clouds.

Primary Emission of Aerosols. Primary aerosols are directly released into the atmosphere following formation via primary emissions from both natural and anthropogenic activities, as discussed in section 1.1.2. Once in the atmosphere, primary aerosols may facilitate secondary aerosol formation, or drive interfacial particle formation by providing surfaces for the condensation of volatile aerosol precursors, often acting as CCN (Seinfeld & Pandis, 2016; Laskin et al., 2015).

1.2.1 Secondary Inorganic Aerosol (SIA). Secondary inorganic aerosols (SIA) arise when gaseous precursors undergo chemical transformation forming low-volatility compounds that condense into the particle phase. This process involves the oxidation of sulfur dioxide (SO_2) and nitrogen oxides (NO_x) into strong acids such as sulfuric acid (H_2SO_4) and nitric acid (HNO_3) (Seinfeld & Pandis, 2016; Kremser, et al., 2016). Due to their low volatility, they partition into the particle phase as liquid droplets under humid conditions in the lower troposphere or crystalize at low humidity in the upper troposphere, where they are readily neutralized by ammonia (NH_3) to form ammonium sulfate or ammonium nitrate salts (Squizzato et al., 2012). The high hygroscopicity of these salts allows them to attract water via hydrogen bond stabilization, making them particularly effective CCN (Seinfeld & Pandis, 2016). Similarly to ice, hydrogen bonds stabilize solid structures, thereby contributing to the incorporation of aerosol precursors into the growing aerosol particulate (Laskin et al., 2015).

1.2.2 Secondary Organic Aerosol (SOA). Similarly to SIA, SOA arise via oxidation of volatile organic compounds (VOCs), which creates oxidation products with low volatility, enabling their condensation into the particle phase (Boucher 2015). The major oxidants involved are hydroxyl radicals (OH) during the day, nitrate radicals (NO_3) at night, and ozone (O_3) reacting with unsaturated VOCs (Zhang et al., 2024). These reactions generate reactive oxygen species (ROS), including highly reactive organic intermediates such as hydroperoxyl radicals (HO_2), peroxy radicals (RO_2), organic peroxides (ROOH), and organic nitrates ($RONO_2$), which subsequently transform into low-volatility products such as organic acids, carbonyls, and multifunctional organics (Chaturvedi et al., 2023; Laskin et al., 2015). Reduced volatility allows these compounds to partition into existing particles, increasing organic aerosol mass, thereby enhancing their ability to act as CCN following further oxidation (Seinfeld & Pandis, 2016).

Another pathway of SOA generation involves aqueous-phase reactions within cloud, fog, or aerosol water. For example, small, water-soluble dicarbonyls, such as glyoxal, dissolve into droplets, where they undergo hydration and further oxidation by aqueous OH radicals, forming non-volatile organic acids (Chen et al., 2018). Under acidic conditions, these compounds can also undergo oligomerization and

react with ammonium, amines, or amino acids, such as glycine, which is frequently observed in atmospheric samples. This results in the formation of nitrogen-containing heterocycles as well as other cyclic compounds characterized by their light absorption, formally classified as BrC chromophores. Acidic sulfate aerosol may further catalyze the formation of organosulfates, adding to SOA mass and altering aerosol hygroscopicity (Laskin et al., 2015).

The complexity of SOA formation pathways produces a chemically diverse mixture of constituents (Laskin et al., 2015), many of which remain poorly characterized (Zhang et al., 2024), highlighting their importance as a continuing area of research.

1.2.3 Heterogeneous & Interfacial Chemistry. Finally, heterogeneous and interfacial chemistry plays a critical role in aerosol growth and aging by modifying composition, volatility, hygroscopicity, and optical properties, frequently yielding additional SOA/BrC mass. Gas molecules can be taken up by pre-existing particles, where they undergo reactions such as the oligomerization of carbonyl compounds in acidic droplets, producing SOA (Laskin et al., 2015; Chen et al., 2018).

Low-volatility vapors can also cluster into stable particles a few nanometers in size while undergoing new particle formation (NPF). NPF is initiated by nucleation of low-volatility vapors, such as sulfuric acid, and stabilized by bases like ammonia or amines, and sometimes by highly oxidized organics (Seinfeld & Pandis, 2016; Kremser et al., 2016); ion-mediated pathways can further lower the activation energy barrier in certain environments, such as stratospheric. While only a small fraction of these initial clusters survive, those that do can grow to sizes capable of acting as CCN (Zhang et al., 2024).

Alongside condensation of vapors and particle–particle coagulation discussed, these surface and bulk aqueous processes govern additional pathways for aerosol growth, lifetime, and their ultimate ability to act as CCN (Laskin et al., 2015; Chen et al., 2018; Chaturvedi et al., 2023).

1.3 Aerosol Optical Properties.

Alongside chemical reactivity leading to atmospheric particle formation and growth, aerosols also impact the climate through their light absorption and scattering (Seinfeld & Pandis, 2016). Aerosols exhibit highly variable optical properties, in how they absorb, scatter, or reflect solar radiation. Optical behavior is strongly dependent on aerosol composition, size, mixing state, and degree of aging (Liu et al., 2015). Radiation emitted by sunlight can interact with atmospheric particles either directly or indirectly, as radiation reflected from earth surfaces is redirected towards higher altitudes. Aerosol light scattering leads to a net cooling effect, as part of the incoming solar radiation is backscattered to space and surface insolation is reduced. In contrast, light absorption causes atmospheric heating because the absorbed shortwave energy is converted to thermal energy within the aerosol layer and subsequently emitted back into the surrounding environment as thermal infrared radiation. The angular distribution of scattered light is set by particle size, shape, and the complex refractive index via Mie scattering; in the geometric-optics limit interpretable as contributions from diffraction, reflection, and refraction (Kokhanovsky, 2008); refraction itself is the deterministic bending governed by the real refractive index and does not by itself send light in all directions. These behaviors, coupled to the formation pathways summarized in Section 1.1.3, control visibility, radiative forcing, and cloud interactions. This section focuses on the optical properties in relation to aerosol type as discussed in previous sections.

Before diving into aerosol absorption, it is important to define radiative forcing (RF); defined as the change in the net balance between incoming solar radiation and outgoing infrared radiation at the top of the atmosphere. Positive RF correlates to a net gain of energy in the Earth system, producing a warming tendency following light absorption, while negative RF signifies a net loss of energy to space, a

cooling tendency, resulting from scattering (Boucher 2015). Absorption and scattering play a key role in RF, though other major contributors, such as greenhouse gases, are also important.

1.3.1 Black Carbon (BC). BC is the most efficient light-absorbing aerosol species, exhibiting broadband absorption across the visible and near-infrared (≈ 400–1000 nm). Internal mixing with non-absorbing coatings, such as sulfates and organics, can enhance absorption, depending on mixing state (Bond et al. 2013). With strong absorptivity and relatively weak wavelength dependence, BC is a major contributor to atmospheric warming, making BC one of the most significant short-lived climate forcers.

1.3.2 Brown Carbon (BrC). Brown carbon refers to a subset of organic aerosol particulates with wavelength dependent absorption strongest in the UV and near-visible range (≈ 300–500 nm). Although BrC is less absorbing than BC, BrC aerosols exhibit more optical activity than most weakly or non-absorbing organic aerosols. Furthermore, BrC is optically distinct from other aerosol light absorbers in that its absorption decreases sharply with increasing wavelength, giving rise to its characteristic "brownish" appearance (Laskin et al., 2015). In addition to altering the radiation budget, BrC provides a sensitive tracer of atmospheric aging processes due to its evolving optical and chemical properties with chemical changes.

1.3.3 Secondary Organic Aerosol (SOA; Weakly and Non-Absorbing Fraction). The majority of secondary organic aerosols are weakly absorbing or primarily light-scattering. Hence these aerosols typically contribute to atmospheric cooling as optically reflective particulates, such as white organics, reflect incoming radiation by increasing planetary albedo (Zhang et al., 2024). However, aqueous-phase SOA chemistry pathways can yield BrC chromophores, imparting selective near-UV and blue-visible absorption (Chen et al., 2018; Laskin et al., 2015).

1.3.4 Mineral Dust and Sea Salt. Mineral dust exhibits mixed optical behavior due to their heterogeneous mineralogy. They primarily scatter visible light but can absorb in the UV and near IR, with optical efficiency depending on particle size, shape, and iron oxide content (Teri et al., 2025). Sea salt aerosols, in contrast, are essentially non-absorbing in the visible and predominantly scattering, especially in clean marine air, enhancing cooling (Schulz et al., 2004).

2. ORGANIC AEROSOL AGING OVERVIEW.

Aerosol aging refers to any chemical or physical transformations occurring after formation that modify particle composition, phase state, volatility, hygroscopicity, and ultimately optical properties. Key atmospheric aging drivers include oxidation by reactive species ($OH/O_3/NO_3$), aqueous-phase reactions in cloud and fog droplets, acid-catalyzed processes in sulfate-rich particles, and heterogeneous surface reactions via gas uptake. Together these pathways alter functional groups and particle morphology, thereby influencing viscosity/phase separation, and can lead to either enhancement or photobleaching of brown-carbon (BrC) absorption (Laskin et al., 2015).

2.1 Oxidative Aging. Oxidative aging is driven by gas-phase oxidants, resulting in either functionalization or fragmentation of condensed-phase organic matter. Atmospheric oxidants driving these two chemical transformation pathways include hydroxyl radicals (OH), ozone (O_3), and nitrate radicals (NO_3).

Functionalization occurs through the addition of oxygen-containing functional groups to organic molecules, such as hydroxyl, carbonyl, carboxylic acid, or peroxides. This generally increases the oxygen-to-carbon ratio (O:C), enhances hygroscopicity, and reduces volatility, thereby increasing the stability of particulates and likelihood of gas-phase aerosol condensation into the particle phase (Kroll et al., 2011).

In contrast, fragmentation involves carbon-carbon bond cleavage, producing smaller, and often more volatile molecules such as carbon monoxide, carbon dioxide, formaldehyde, and acetaldehyde. Fragmentation tends to reduce aerosol mass, shortening particle lifetime (Kroll et al., 2011).
The oxidation reaction pathway depends on the oxidation state of the aerosol, with the initial stages of oxidation favoring functionalization and later stages favoring fragmentation of highly oxidized compounds (Kroll et al., 2011).

Oxidative aging alters the balance between light scattering and absorption. The addition of groups via functionalization generally increases particle scattering through enhanced hygroscopic growth, producing a negative RF. Fragmentation, reducing mass and particle size, can reduce aerosol lifetime and optical efficiency; producing positive RF in highly oxidized compounds in reducing scattering and increasing absorption; while fragmentation of compounds at lower oxidation states reduces aerosol mass and optical activity altogether (Liu et al., 2014).

2.2 Aqueous-Phase Aging. Aqueous-phase aging involves chemical transformations that occur in liquid water associated with clouds, fog, or deliquesced aerosol particles. This provides a highly soluble environment for polar organics, enabling condensed-phase reaction pathways otherwise unavailable in the gas phase (Ervens et al., 2011; McNeill, 2015).

A key class of precursors for aqueous aging are small, water-soluble carbonyls such as glyoxal and methylglyoxal. Once dissolved, these compounds undergo hydration to form gem-diols, aldol condensation to produce oligomers, and acetal formation in the presence of alcohols. In addition, aqueous oxidation by OH and HO_2 radicals produces low-volatility products such as oxalic acid and other dicarboxylic acids, increasing aerosol mass, which contribute substantially to aqueous secondary organic aerosol (aqSOA) mass (Ervens et al., 2011).

Ammonium-mediated aging of SOA can lead to the formation of nitrogen-containing chromophores with imidazole-like structures that absorb strongly in the near-UV and visible range (Bones et al., 2010). These products act as brown carbon (BrC) chromophores, imparting strong light absorption in the near-UV and visible ranges.

These reactions can either increase light absorption, by forming conjugated chromophores, or reduce it through oxidative bleaching. Oligomerization and nitrogen-containing chromophore formation enhance BrC absorption, resulting in positive RF. Conversely, advanced oxidation can degrade chromophores and lead to photobleaching, shifting the radiative impact toward cooling in decreasing absorption (Laskin et al., 2015).

2.3 Heterogeneous Processes. Heterogeneous reactions occur directly at the interface between gases and aerosol particle surfaces, often involving trace gases. Unlike aqueous-phase aging, which takes place in bulk liquid water, these transformations are restricted to the particle surface, where gas uptake rates and microenvironmental conditions strongly influence reaction efficiency (George & Abbatt, 2010).

Several trace gases participate in heterogeneous uptake. For example, the uptake of nitrogen oxides (NO_2, N_2O_5) by organic-rich particles promotes nitration and organonitrate formation. These reactions introduce nitro ($–NO_2$) and nitrate ester ($–ONO_2$) functionalities, often onto aromatic systems, resulting in the formation of nitroaromatics and organonitrates, which act as strong brown carbon (BrC) chromophores (Laskin et al., 2015).

In acidic or sulfate-rich environments, oxidative SO_2 uptake yields organosulfates through acid-catalyzed reactions with alcohols, polyols, or epoxides. The incorporation of sulfate ester groups ($–OSO_3^-$) increases particle polarity and hygroscopicity, leading to greater water uptake and CCN activity (Surratt et al., 2008).

Ozone reacts with unsaturated organic bonds through ozonolysis, cleaving double bonds and forming smaller, oxygenated products such as carbonyls and carboxylic acids. These reactions may also occur in the aqueous phase. However, they differ from direct oxidative aging by ozone (radical-driven pathways) discussed previously, because they often proceed via ozonolysis followed by oligomerization mechanisms. Instead of primarily producing small oxidized species, these reactions generate larger, low-volatility oligomers, although oxygen-containing functional groups can also be incorporated during the process (Niu et al., 2020).

The optical consequences of heterogeneous surface chemistry vary strongly by reaction pathway. Reactive uptake of nitrogen oxides produces nitroaromatics and organonitrates, both of which are efficient brown carbon chromophores that enhance near-UV and visible absorption, driving positive RF. In contrast, SO_2 uptake generates organosulfates that, while weakly absorbing, increase aerosol polarity and hygroscopicity, thereby strengthening light scattering and contributing to negative RF. By contrast, ozone uptake via ozonolysis cleaves unsaturated bonds thereby degrading conjugated chromophores, resulting in photobleaching of BrC and reduced absorption (Laskin et al., 2015).

3. INTRODUCTION TO STRATOSPHERIC BrC AGING.

A study on sulfate aerosols found a correlation between global climate and volcanic eruptions (Robock 2000). Following large scale volcanic eruptions, a net negative radiative forcing was observed, with global temperatures falling by ~0.5 °C after 8 months, gradually returning to baseline after 1-3 years (Soden et at., 2002). Robock's work supports this observation, suggesting that sulfate aerosol formation may drive global cooling following major volcanic events. Oxidation of volcanic SO_2 by OH radicals generates SO_3, which subsequently hydrates into sulfuric acid. These low-volatility products condense into droplets, enabling effective light scattering due to their size and optical properties, while also providing an interface for multiphase chemical processes (Robock 2000).

3.1 The Stratospheric Environment. The stratospheric environment is characterized by low pressures and temperatures, with temperatures reaching -80°C and pressures as low as 0.001 atm (Karl et al., 1999). Higher altitudes are also associated with a systematic decrease in relative humidity, as water molecules at higher elevations mainly originate from tropopause transport and methane oxidation, resulting in relatively negligible, though non-zero, vapor pressures (National Aeronautics and Space Administration, 2021; solomon et al., 2010). Under such low pressure and temperature conditions, the limited water molecules present in the stratosphere either participate in ice nucleation on solid surfaces, or partition into surrounding liquid droplets, forming supercooled aqueous droplets via hydrogen bonding interactions with surrounding polar molecules (Roy et al., 2023). Thus, deposition into sulfuric acid droplets is expected with molecules that can participate in intermolecular force interactions, including bisulfates, sulfur trioxide, amines and ozone, diversifying possible reaction pathways with varying global implications.

3.2 Stratospheric Implications of Volcanic Eruptions. Unlike typical volcanic eruptions which lead to global cooling, studies on the 2022 Hunga Tonga–Hunga Ha'apai found an increase in RF activity. The submarine eruption injected ~146 Tg of water vapor into the stratosphere, increasing the total stratospheric water content by ~10% (Millán et al., 2022). The co-emission of SO_2 and water vapor facilitated the formation of larger, more dilute sulfuric acid droplets, which persisted longer and scattered solar radiation more efficiently. This enhanced scattering contributed to global cooling, while the increased particle size also led to localized warming in the lower stratosphere due to absorption of terrestrial infrared radiation by larger sulfate particles that settle downward (Zhu et al., 2020; Li et al.,

2022; Chen et al., 2025). In contrast, under more concentrated acidic conditions typical of the stratosphere (~70–80 wt% H_2SO_4), the reduced water content may favor acid-catalyzed pathways such as dehydration, esterification, and fragmentation, producing small, light-absorbing organic and inorganic species (Sicard et al., 2023). Such products could increase aerosol absorption of radiation, potentially offsetting or counteracting scattering-driven cooling with localized stratospheric warming, though the magnitude of this effect, and humidity influences, remain uncertain.

3.3 Stratospheric Aerosol Formation. As discussed in section 1.1, volcanic events may result in the formation of primary carbonaceous and inorganic aerosols (sections 1.1.4 and 1.1.6., respectively). As discussed, combustion generates primary organic carbon aerosols, including BrC, as well as SOA precursors in the form of VOCs. Meanwhile, SO_2 released during volcanic eruptions is oxidized into sulfuric acid, playing an important role in SIA formation, and potentially in acid-catalyzed SOA pathways (Jang et al., 2001).

While aerosol formation is well understood, SOA, SIA, and heterogenous aging processes remain poorly characterized in highly acidic conditions (Surratt, et al., 2008). In previous studies, sulfuric acid droplet formation has been directly linked with the partitioning of VOCs into the liquid phase (Lin et al., 2012; Jang et al., 2001). However, these studies primarily focus on ammonium aerosol formation processes, or SOA formation under mildly acidic conditions (Guo et al., 2015; Altieri et al., 2008). Thus little is known about stratospheric aging processes where nucleophiles like ammonia, which are instrumental in ammonium aerosol formation, are absent; as they are quickly protonated in highly acidic environments (Pye et al., 2020). On the other hand, many SOA formation mechanisms rely on aqueous phase processes, thus it remains unclear whether highly acidic conditions will favor organosulfate formation (Surratt, et al., 2008; Tolocka et al., 2004) or prevent it in inhibiting oligomerization (Cooke, et al., 2024). Furthermore, work on oxidative SOA processes support the formation of organic acids, carbonyls, and multifunctional organics, though it is unclear which subsequent reaction pathways are underway (Surratt, et al., 2008); these products are often understood to yield organosulfates and oligomers, yet stratospheric conditions may suppress such pathways, leaving open the possibility that these VOCs either remain volatile, undergo further oxidation, or participate in alternative acid-catalyzed transformations (Surratt et al., 2010). Moreover, the role of heterogeneous chemistry under highly acidic conditions in the stratosphere is poorly understood, emphasizing the need for further investigation into stratospheric SOA formation (Hanson et al., 1994). In an attempt to bridge this gap, this next section primarily focuses on potential stratospheric acid-catalyzed pathways underway.

3.4 Acid Catalyzed BrC Aging Mechanisms. Acidic conditions can drive the formation of numerous products, though reaction pathways strongly depend on the chemical environment. This thesis investigates BrC aging under stratospheric conditions, thus this section will focus on acid catalyzed pathways under strongly acidic conditions (pH < 1).

Sulfuric acid particulates, formed from gaseous precursors released through volcanic eruptions, tend to cluster into weakly hydrated droplets (~75 wt% H_2SO_4); as low pressure and temperatures prevent the accumulation of many compounds in this environment. Under such conditions, the formation of acetals, oligomers, esters, and anhydrides is favored (Zhu et al., 2022; Jang et al., 2002). Carbonyls, alcohols and polyols may undergo nucleophilic substitution [1] forming acetals, as low water conditions suppress hemiacetyl formation; though it is important to note that acetal formation is limited by stratospheric alcohol availability, and thus potentially suppressed. Though stratospheric alcohol availability and acetal formation is not heavily researched or understood, remaining speculative. However, alongside organic acids, alcohols and polyols may also undergo esterification [2] forming

organic esters. Carboxylic acids and alcohols can participate in dehydration [3] pathways as well, generating acid anhydrides, especially in the absence of nucleophiles, as substitution pathways are suppressed. Oppositely, dehydration of sugars [4] under such low water conditions result in HMF and furfurals that can polymerize into humins-like oligomers. Though, oligomerization under acidic conditions is not strictly reserved for dehydration driven pathways alone, as resinization [5] and aldol condensation [6] pathways may proceed under strongly acidic conditions; forming phenolic oligomers from phenolics and small aldehydes [5], or aldol oligomers from enolizable carbonyls [6], respectively. Moreover, polymerization [7] of unsaturated alkenes and trepenes may occur, yielding C-C linked oligomers, though limited by the presence of olefins available to react in BBOA (Fleming et al., 2020). Resinization, polymerization, and aldol condensation pathways are possible, though less favored under stratospheric conditions as such pathways are hydration state independent, thus dehydration and acetylation pathways are favored under such low water conditions.

Other potential reaction pathways may form organosulfates, aromatics, and oxygenated compounds, though such pathways are dependent on the presence of other reactive species. In the presence of sulfates or bisulfates, alcohols and phenols may undergo sulfation (esterification) pathways [8] forming organosulfates. Sulfur trioxide under strongly acidic conditions drives the formation of aryl-sulfonic acids and sulfonates from aromatic precursors [9]. Conversely, in the presence of nitronium, aromatics tend to form nitro-aromatic compounds [10] (Fleming et al., 2020). Thus, sulfonate and nitro-aromatic formation equilibrium is strongly dependent on stratospheric sulfur trioxide and HNO3/NO_x availability.

Aside from acid catalyzed reactions, strongly acidic conditions enable oxidative and electrophilic substitution pathways. Low water conditions alongside ozone uptake leads to ozonolysis [11] of alkenes and unsaturated aromatics, generating small oxygenates. Acidic conditions also allow for imidazole formation [12] of amines by unprotonated amines. However, strongly acidic conditions (pH < 1) tend to suppress such pathways due to lack of available nucleophiles, as they are rapidly protonated.

[1]–[12] refer to acid-catalyzed mechanisms described in Carey and Sundberg (2007).

3.5 Experimental Introduction to Stratospheric Acid Catalyzed Aging. Guided by the mechanisms above, the present experiments use low pH-controlled sulfate matrices to quantify how sulfuric acid rich conditions regulate acid catalyzed BrC formation. As discussed in section 1., aerosol formation pathways, including Aldol condensation, Sulfation, Ozonolysis, and Imidization may also play a role in stratospheric aerosol aging mechanisms discussed in section 3.4, which leads to the question of whether sulfuric acid aging may generate BrC via SOA mechanisms guiding carbonaceous BrC formation. The objective of this study is to characterize the molecular and optical changes in BBOA following acid-catalyzed aging under simulated stratospheric conditions. Understanding these aging mechanisms is critical for improving climate models, as BrC optical properties influence RF and atmospheric lifetime.

To investigate whether sulfuric acid-rich stratospheric conditions promote BrC formation via acid-catalyzed SOA pathways, this study investigates aged BBOA in simulated stratospheric matrices. BBOA samples were extracted into either water or concentrated sulfuric acid (16 M H_2SO_4) and incubated in the dark for 24 hours to mimic nighttime aging. Post-aging, samples were neutralized and analyzed using UV-Visible spectroscopy, wavelength-resolved absorption photodiode array detection (PDA), and LC–ESI–MS to quantify changes in optical properties and molecular composition. Mass spectrometry data was processed using homologous series extension calculations in RStudio (Schum et al., 2020) to assign molecular formulas and identify structural trends in aged aerosol products; analysis focused on

aerosol structural properties to uncover potential acid-catalyzed formation and aging pathways. This approach allows for direct assessment of how extreme acidity influences BrC evolution in volcanic stratospheric aerosols.

4. MATERIALS AND METHODS

4.1 Sample Extraction. BBOA coated (~3-4 mg) quartz slides were received from the University of British Columbia (UBC) and extracted in either water, for aqueous phase acid catalyzed aging, or 16 M H_2SO_4 for acid catalyzed aging in sulfonated water droplets. Extraction solvents were placed in an ice bath in preparation, though extractions were completed on the benchtop at ambient temperature. BBOA extraction involved placing the slide at the bottom of a glass vial prior to solvent addition. However, degradation of organic material was observed in some trials where the slide landed face down in the vail, producing black material. Furthermore, under such circumstances BBOA, would remain stuck between the bottom of the vail and quarts slide, leading to inconsistent BBOA content across samples. For consistency across multiple experiments and retention of aging products, solvent was placed into the vial, followed by addition of the slide and immediate capping. Samples were placed on the shaker for ~10 minutes for near-complete BBOA extraction. The water extracted BBOA samples were treated with 16 M H_2SO_4 immediately following extraction by dilution with an 18 M stock H_2SO_4 solution.

4.2 Aging & Incubation. BBOA night time aging was simulated by placing samples in a dark room for 1 day. Samples were placed in a dark drawer immediately following extraction on the shaker and initial UV/Vis measurements, and were removed after 24 hours for aged UV/Vis measurements, followed by immediate neutralization.

4.3 Neutralization. Neutralization of acidic samples was necessary for LCMS analysis and solvent separation in liquid-liquid extractions. Samples were placed in an ice bath during the neutralization procedure to prevent thermal degradation. In order to prevent inaccurate pH paper readings, water was used to dilute solution upon K_2SO_4 solid formation, and samples were fitted with a flat teflon stir bar. A 20 M potassium hydroxide (KOH) stock solution was used to neutralize the sample mixture in 100 μL increments. Once a pH of 2 was reached, a 10 M potassium hydroxide (KOH) stock solution was added in 50 to 100 μL increments until a pH of 3 was reached.

4.4 Extraction with Organic Solvent. A liquid-liquid extraction was performed in order to isolate BBOA aging products from the aqueous salts formed during neutralization. Ethyl acetate was chosen as the extraction solvent for collection of the organic aging products. The water fraction was extracted three times, and the resulting ethyl acetate fractions were combined. A sealable glass vial with a teflon cap was chosen as the extraction chamber in order to induce BBOA partitioning into the organic phase by shaking. The organic phase was isolated from the extraction chamber using a 10 mL micropipette to prevent salts accumulation in the organic phase, as observed once flowing through a separatory funnel.

4.5 LCMS Sample Preparation. BBOA aging products were isolated by removing the ethyl acetate solvent via rotary evaporation to dryness. The rotovap was set to ~300 rpm and 32°C (the relatively low T was chosen to prevent loss of volatile organic products during evaporation). The resulting products were redissolved in a 1:1 mixture of HPLC grade nanopure water acetonitrile solution (MS solvent). Impurities were removed using a 0.2 μm hydrophilic PTFE syringe filter (Millex-LG, MilliporeSigma) pre-treated with MS solvent.

4.6 Quality Controls. Experimental quality controls included three blank solutions (B1, B2, B3) and three control samples (V2, V22, V44). Experimental blanks included an MS solvent blank (B1),

extracted MS solvent blank (B2) and a neutralized MS solvent blank (B3). B1 was prepared by combining equal parts of HPLC grade nanopure water and acetonitrile. B2 was prepared by extracting HPLC grade nanopure water in ethyl acetate, followed by solvent evaporation to dryness. B2 was redissolved in the MS solvent and pushed through a filter syringe. B3 was prepared by neutralizing 16 M SA, following the same procedures for organic solvent extraction and MS sample preparation as outlined for the experimental sample preparation.

Samples extracted directly in sulfuric acid, as opposed to water, contained a greater initial BBOA concentration, thus three controls were used for each trail. V2 and V22 were prepared alongside the WS BBOA aged sample, as equal volumes of a water extracted BBOA solution were separated into three vials. The samples were diluted with water as opposed to sulfuric acid. The first control (V2) was diluted in acetonitrile for a 1:1 HPLC grade nanopure water acetonitrile solution. The second control (V22) was extracted in ethyl acetate, following the extraction and LCMS preparation procedures used for the water extracted aged sample sample. The BBOA control (V44) for the sulfuric acid extracted sample was prepared in a similar manner to V22, with one deviation, as a greater volume of the water-extracted BBOA solution was used to match the BBOA concentration of the total BBOA aged sample. Following dilution, V44 was prepared following the V22 preparation procedure.

4.7 UV-Visible Spectroscopy. UV-Visible absorbance spectra were collected immediately following BBOA extraction and repeated after 24 hours of aging. Blanks were prepared using the corresponding solvent for each sample type; a 16 M H_2SO_4 solution was the chosen blank for UV/Vis measurements of acid-treated samples, while a water blank was used for controls. Samples were transferred to quartz cuvettes with a 10 mm path length for absorbance measurements. Spectra were recorded on a Shimadzu UV-2450 UV-Vis spectrometer equipped with UVProbe software over the 200–700 nm range, with analysis focused on 300–650 nm.

4.8 Mass Spectrometry. Samples for mass spectrometry were prepared by dissolving in a 1:1 volume ratio of water and acetonitrile (ACN). Large and insoluble particles were removed by filtration through a 0.2 μm hydrophilic PTFE syringe filter (Millex-LG, MilliporeSigma) to protect the instrument. Blanks consisted of 1:1 water:ACN solvent and filtered solvent blanks. Experimental controls included an untreated BBOA sample dissolved in 1:1 water:ACN, the same BBOA sample extracted with ethyl acetate prior to dissolution, and a sulfuric acid only control. Samples were analyzed in both positive and negative electrospray ionization modes.

Orbitrap output data was processed in Rstudio using molecular formula assignment software (Schum et al., 2020). MS data analysis involved PDA plots generated in the Qual browser of Xcaliber to determine the retention time (RT) of chromophores at the orbitrap photodiode detector. The time laps between the orbitrap photodiode detector and MS detector was corrected by adding 0.06 s to RT's found in Xcaliber. MZmine was then utilized to match m/z values with their corresponding MS RT's. Single ion chromatograms for each m/z value at each respective RT were checked in freestyle to identify chromophore m/z values. Predator formula calculator and Rstudio MSassignR outputs were compared and formulas with the most plausible DBE values and elemental ratios were chosen for m/z formula assignments.

5. RESULTS: ACID CATALYZED AGING MOLECULAR COMPOSITION IMPLICATIONS

A comprehensive analysis across multiple compositional metrics suggests sulfuric acid aging produced new sulfur and nitrogen containing compounds with high DBE and elevated O/C, consistent

with the formation of light-absorbing BrC chromophores such as conjugated carbonyl/phenolic oligomers and organosulfate-bearing species. UV–Vis spectra confirmed that these transformations translated into measurable optical effects, with enhanced absorbance within the 300–500 nm range.

Water extraction reduced the contribution of sulfur- and nitrogen-containing species, highlighting that extraction methodology strongly influences observed BrC composition. Nonetheless, both acid-treated pathways clearly demonstrated that sulfuric acid catalysis is a major driver for secondary BrC formation from BBOA.

5.1 UV/Vis Spectra. The first set of UV/Vis experiments aimed to investigate the hydration state dependence of acid catalyzed BrC formation. This was achieved by comparing absorbance (a.u.) across 4 different samples: WS BBOA aged in 10M H_2SO_4, Total BBOA aged in 10M H_2SO_4, WS BBOA aged in 16M H_2SO_4 and Total BBOA aged in 16M H_2SO_4 as illustrated in figure 1. The experimental control was unaged BBOA extracted in water, which was also used to prepare each experimental sample via serial dilutions in 18M sulfuric acid. Thus it is important to note that the BBOA concentration was not standardized across samples, as the 10M H_2SO_4 treated samples were prepared via a 2 fold dilution of the control, while the 16M H_2SO_4 treated samples involved a 10 fold dilution. Nevertheless, samples treated with highly concentrated acid exhibited a significant increase in absorption within the 300-500 nm region following 24 hours of aging, with the most profound enhancement observed in H_2SO_4 extracted samples. Samples treated with more dilute H_2SO_4 concentrations showed a much less profound change in absorbance intensity within the visible and near visible region, with a similar trend across samples as water extracted samples treated with 10 M H_2SO_4 showed a much less profound change in absorption as compared to H_2SO_4 extracted samples.

Interestingly, samples treated with the more concentrated acid showed absorbance maxima at around 350 nm and 375 nm, absent in the less concentrated acid-treated samples. despite the 5 fold difference in BBOA content. These wavelengths fall in the canonical BrC window (300–500 nm), typical of conjugated carbonyl/phenolic oligomers, likely formed via dehydration pathways. These results indicate that acid catalyzed BrC formation is likely hydration state dependent, reflecting that the formation of chromophores in highly acidic environments, such as the stratosphere, are governed by different reaction pathways than those observed with more hydrated sulfate aerosol droplets found at lower altitudes. Thus, 16 M approximates poorly hydrated stratospheric sulfate aerosols, while 10 M represents a more hydrated UT/LS endmember, consistent with weaker BrC production at 10 M.

The next set of UV/Vis experiments aimed to investigate acid catalyzed BrC formation time dependence by comparing unaged BBOA with both total and WS BBOA after 24 hours of aging, as well as total BBOA after 1 week of aging (see figure 2). Sample preparation followed the same procedure as previous experiments, with the experimental sample 10 times more dilute than the control. Although 24 hr experiments showed consistent absorption enhancement in the total BBOA fraction, as in previous experiments, further aging to 1 week produced anomalous increases in the total BBOA fraction. These absorption changes are likely laboratory artifacts of extended exposure to concentrated H_2SO_4 under static, closed conditions, as atmospheric sulfate aerosols are subject to continuous dilution, gas exchange, and photolysis; thus, such long-term static reactions are unlikely to be environmentally relevant. Our results therefore suggest that the dominant acid-driven pathways occur on short timescales (<1 day), with little evidence for progressive changes over extended durations under stratospherically relevant conditions. Following this finding, proceeding experiments were performed over a 24 hour aging period.

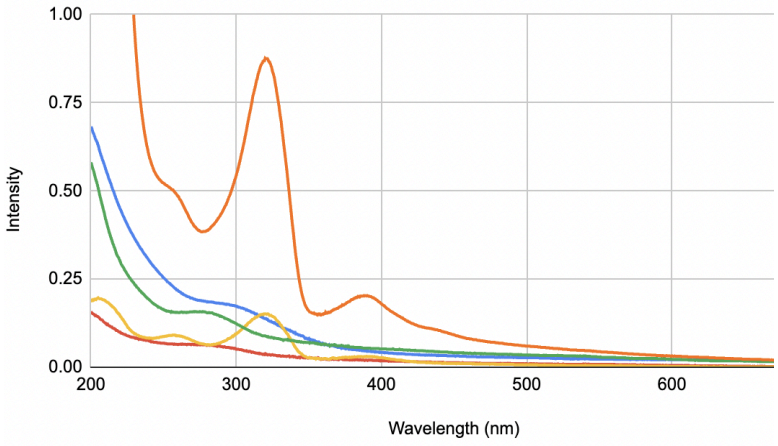

Figure 1: Hydration State Dependence UV/Vis Spectra. Absorption intensity wavelength dependence of 24 hour aged BBOA across varying acid concentrations and extraction procedures, including: WS BBOA aged in 10M H_2SO_4 (red), Total BBOA aged in 10M H_2SO_4 (green), WS BBOA aged in 16 M H_2SO_4 (yellow), Total BBOA aged in 16 M H_2SO_4 (orange), and an unaged BBOA control (blue) with colors indicating sample identity. Values are reported as absorbance (a.u.), normalized to path length with baseline subtraction.

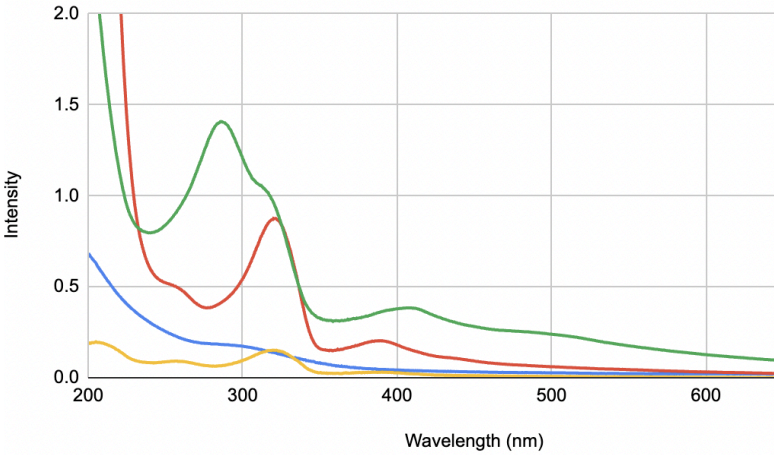

Figure 2: Time Resolved UV/Vis Spectra. Absorption intensity wavelength dependence of aged BBOA across varying aging time periods and extraction procedures, including: WS BBOA after 24 hours of aging in 16M H_2SO_4 (yellow), Total BBOA after 24 hours (red) and 1 week (green) of aging in 16M H_2SO_4, and unaged BBOA (blue), with colors indicating sample identity. Values are reported as absorbance (a.u.), normalized to path length with baseline subtraction.

5.2 Molecular Composition of Control vs. Acid-Aged BBOA. Double bond equivalent (DBE) versus carbon number distributions are compared in figure 3 for both untreated BBOA (3a) and sulfuric acid aged BBOA under two extraction conditions; water-extracted (3b) and acid-extracted (3c). Control samples exhibited primarily CHO and CHNO compounds centered at DBE values of 0–10 and carbon numbers between 10–30. Sulfur- and nitrogen-containing species, including CHNOS, CHOS, CHNS, CHS and CHN, were largely absent in the control, as expected with unprocessed, resin-free biomass burning emissions.

In contrast, both acid-treated samples showed expanded distributions of CHOS and CHNOS containing species, along with a shift toward higher DBE values at similar carbon numbers. This indicates incorporation of sulfate groups and enhanced aromaticity. There is also a notable change in the oxygen to carbon ratio with greater carbon numbers, indicating that larger molecules lose oxygen functionality under acid treatment, while smaller molecules gain oxygen through addition reactions.

Furthermore, the formation of smaller oxygenated compounds and an increase in the oxygen to carbon ratio is observed at lower carbon numbers and DBE values, further suggesting oxygen addition via acid-catalyzed pathways such as sulfation, esterification, or acetalization. Notably, sulfuric acid extracted BBOA produced a broader distribution of CHNO compounds, suggesting enhanced stability of aromatic reaction pathways or accumulation of nitrogen-containing products under strongly acidic conditions.

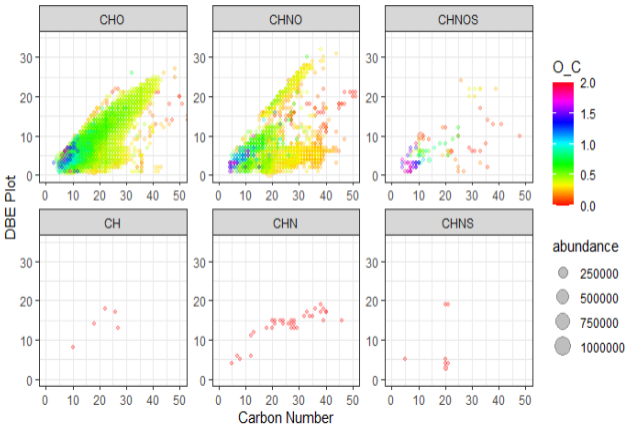

Figure 3a: Untreated BBOA

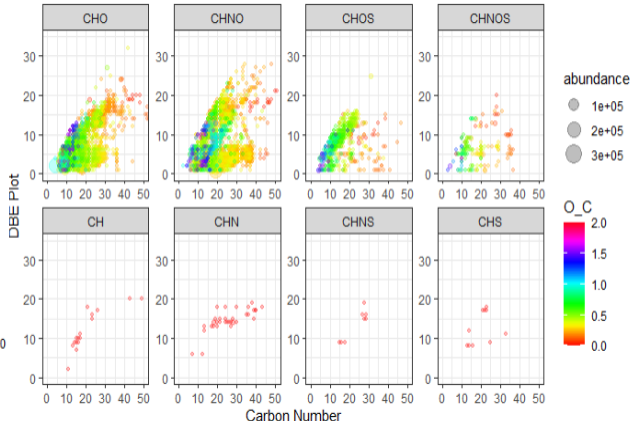

Figure 3b: WS BBOA Aged

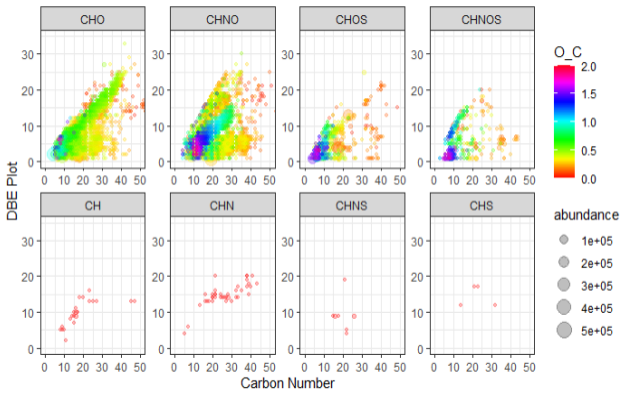

Figure 3c: Total BBOA Aged

Figure 3: DBE vs. Carbon Number indicates the degree of saturation of unaged BBOA (top left) and sulfuric acid treated experiments: water extracted BBOA (right) and sulfuric acid extracted BBOA (bottom). Clusters indicate chemically similar compounds while color intensity corresponds to the degree of oxidation.

5.3 Elemental Ratios and Degree of Unsaturation. The van Krevelen diagrams provide additional insight into the oxidation states of control versus acid-aged BBOA (Figure 4). The untreated BBOA control (4a) showed a relatively narrow O/C (<1.0) distribution and H/C values centered near 0.0–0.75, consistent with moderately oxidized organics. Acid-treated samples, however, displayed a substantial increase in O/C (>1.0) and a spread of H/C values centered near 0.0–2.0, suggesting the formation of more oxygenated, unsaturated products.

Moreover, a substantial decrease in DBE values is observed at higher H/C ratios; meanwhile, high DBE values cluster at lower H/C ratios, especially in highly oxygenated compounds, further supporting the formation of more oxygenated, unsaturated products. Importantly, the acid-extracted sample (3c) showed clustering of high-DBE CHNO and CHNOS species at low H/C (<1.0), consistent with polyaromatic and conjugated nitrogen/sulfur functionalities. Such structures are strongly light-absorbing, consistent with brown carbon chromophores. The water-extracted sample exhibited a comparatively broader spread in O/C and less clustering at high DBE, consistent with more moderately oxidized BrC.

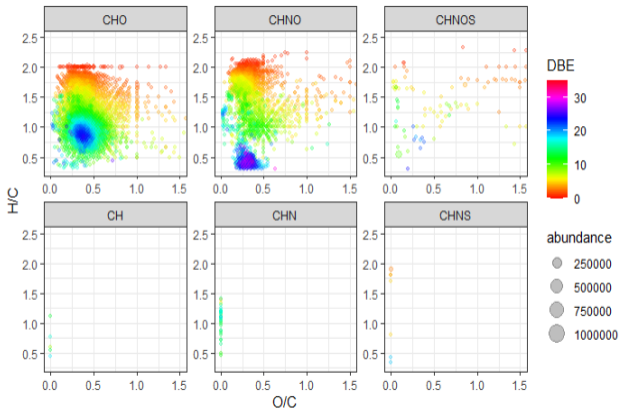

Figure 4a: Untreated BBOA

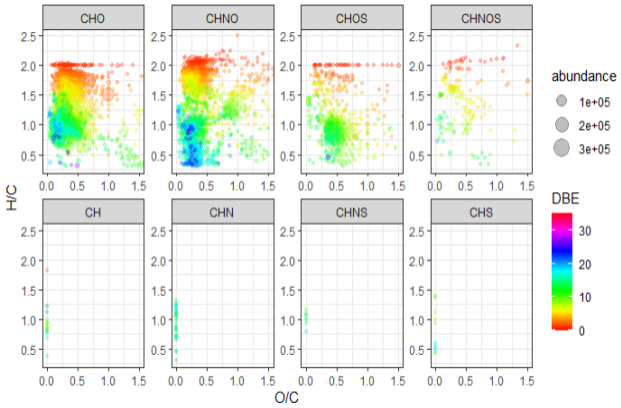

Figure 4b: WS BBOA Aged

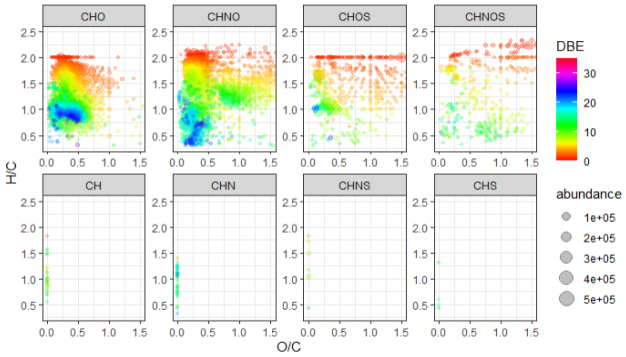

Figure 4c: Total BBOA Aged

Figure 4: H/C vs. O/C Rations indicate the degree of oxidation and saturation, or aromaticity, in the untreated BBOA (4a), WS BBOA aged (3b) and Total BBOA aged (3c). Clusters indicate chemically similar compounds while color intensity corresponds with saturation.

5.4 Carbon Number and Atomic Number Distributions. Carbon number trends are summarized in Figure 5. The untreated-aged control BBOA displayed primarily CHO and CHNO species centered around C_{15}–C_{25}, with limited sulfur incorporation. Upon sulfuric acid treatment, the distributions shifted toward higher numbers of sulfur- and nitrogen-containing species (CHOS, CHNOS, CHNS), particularly at C_{10}–C_{20}. The water-extracted sample showed enhanced contributions from CHOS species, whereas the acid-extracted sample retained a stronger CHNOS distribution, and species with greater carbon content.

These observations suggest that sulfuric acid catalysis not only promotes sulfation but also facilitates the incorporation of nitrogen containing species. The differences in extraction reflect partitioning behavior, with water extraction preferentially retaining polar organosulfates, while direct acid extraction preserves less polar, conjugated nitrogen-containing species.

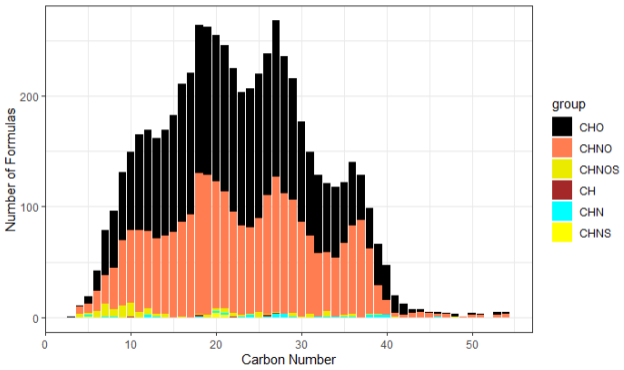

Figure 5a: Untreated BBOA

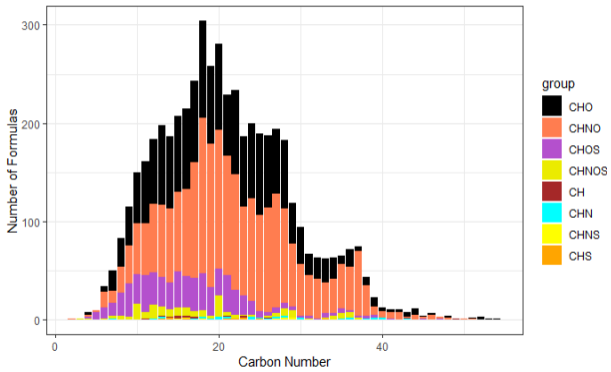

Figure 5b: WS BBOA Aged

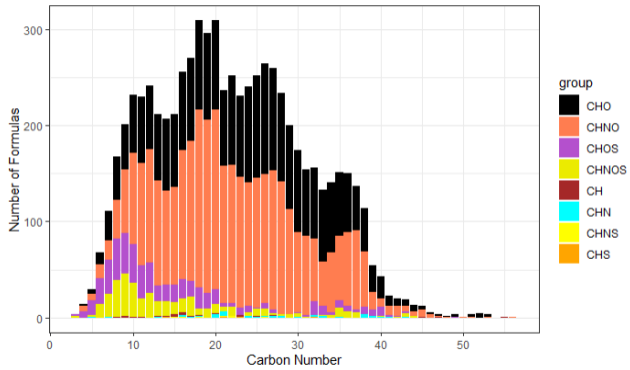

Figure 5c: Total BBOA Aged

Figure 5: Aged Product Distributions in Relation to Carbon Content. Colors indicate different chemical families, with color distribution across the y-axis corresponding to the relative abundance of a chemical family among compounds of equal carbon content, hence similar in size.

5.5 Oxygen Number Distributions. Oxygen number distributions across molecular classes are summarized in figure 6. The untreated-aged BBOA control exhibited formulas containing 5–10 oxygen atoms on average, typical of moderately oxidized biomass burning organics. Acid-aged samples showed a pronounced shift toward higher oxygen numbers (10–20), with enhanced contributions from CHOS and CHNOS species.

The water-extracted sample demonstrated formation of high oxygen containing species, suggesting enrichment in organosulfates and carboxylic acids. By contrast, the acid-extracted sample retained a broader mix of moderately oxygenated CHNO compounds as well as a shift towards highly oxygenated compounds, highlighting a balance between oxidation and reduction pathways. These findings suggest that while acid catalysis broadly increases oxidation, the extraction method dictates the extent of reduction pathways.

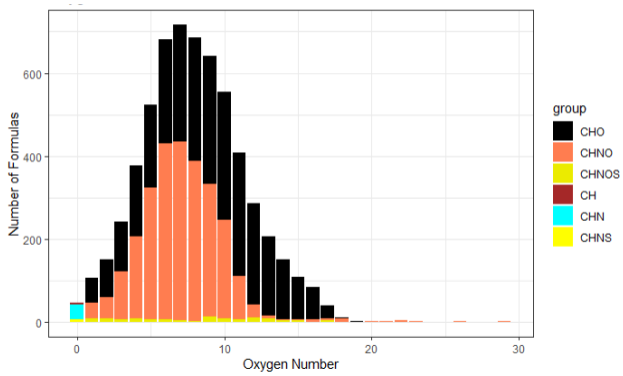

Figure 6a: Untreated BBOA

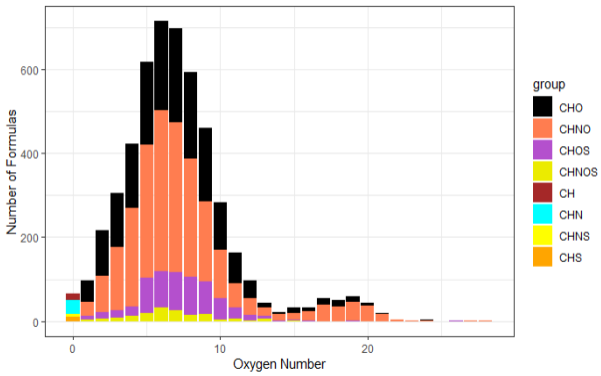

Figure 6b: WS BBOA Aged

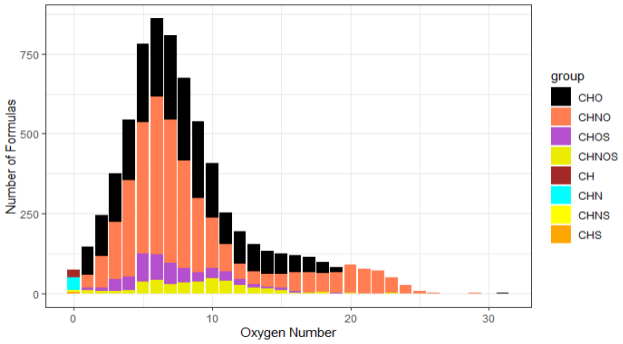

Figure 6c: Total BBOA Aged

Figure 6: Aged Product Distributions in Relation to Oxygen Content. Colors indicate different chemical families, with color distribution across the y-axis corresponding to the relative abundance of a chemical family among compounds with equal oxygen content, hence, similar in oxidation state.

5.6 Optical Signatures of Acid-Catalyzed BrC Formation. PDA spectra confirmed that these compositional changes translated into measurable optical effects. Acid-treated samples exhibited enhanced absorbance within the 300–500 nm range with visible chromophore formation, especially at later retention times, suggesting formation of conjugated carbonyl/phenolic oligomers and organosulfates; as nitroaromatics would require NOx and imidazoles unprotonated amines, which are not confirmed under these conditions. Water-extracted samples showed fewer chromophores in comparison to the sulfuric acid extracted samples, likely resulting from stronger scattering signatures due to increased polarity and hygroscopicity. Meanwhile, acid-extracted samples exhibited more pronounced absorption features, attributable to highly conjugated chromophores, as well as strong absorption near 300 nm across a broad retention time range, suggesting crosslinking acid catalyzed pathways.

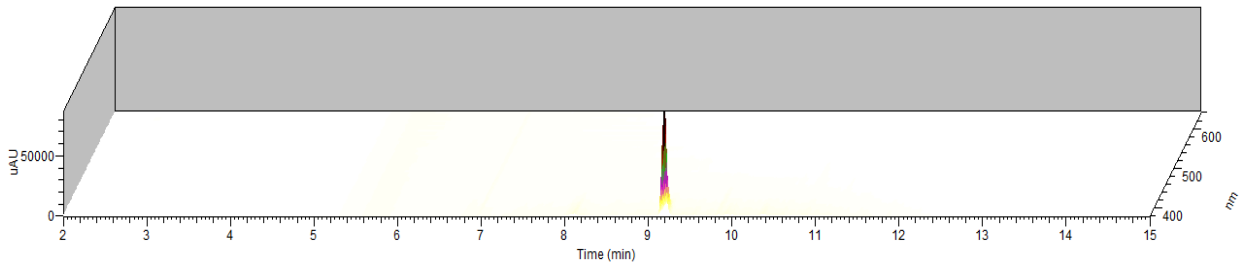

Figure 7a: Untreated BBOA

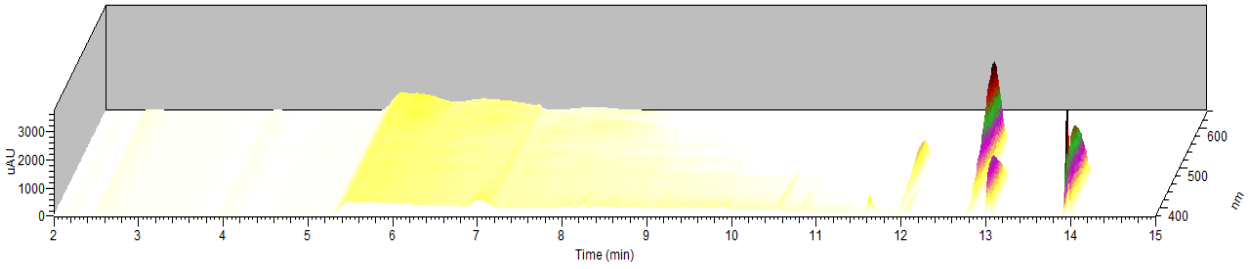

Figure 7b: WS BBOA Aged

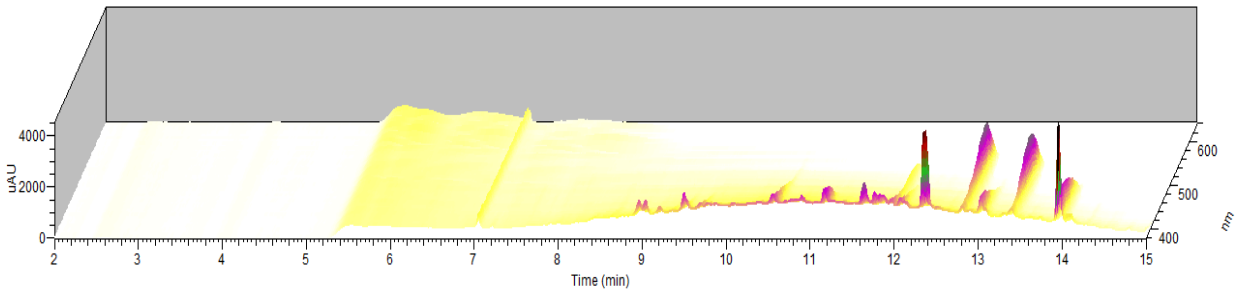

Figure 7c: Total BBOA Aged

Figure 7: 3D PDA Plots illustrate changes in absorption intensity over wavelengths of 380 - 640 nm and a retention time range of 2-15 minutes across three different samples: untreated BBOA (top panel), water extracted-sulfuric acid aged BBOA (middle), and sulfuric acid extracted and aged BBOA (bottom). Taller peaks with darker colors indicate higher relative absorption intensities across their corresponding wavelengths and retention times.

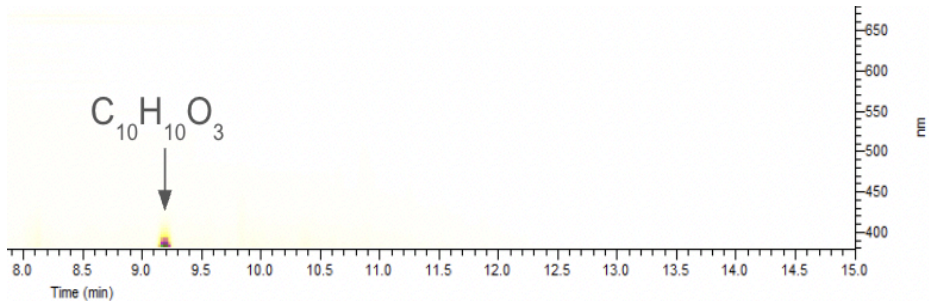

Figure 8a: Untreated BBOA

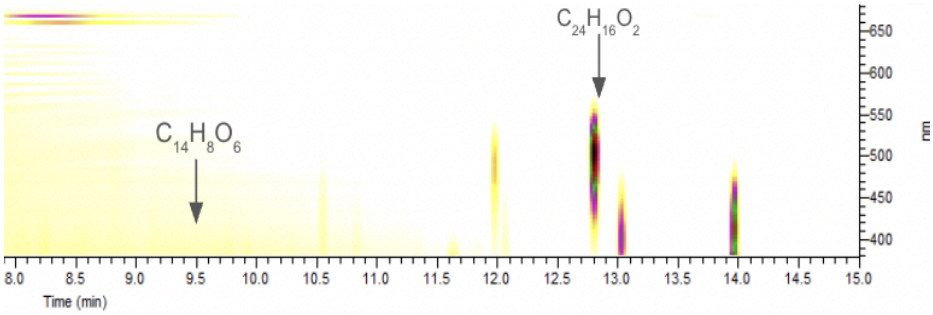

Figure 8b: WS BBOA Aged

Figure 8: 2D PDA Plots of Identified Chromophores illustrates absorbance intensity with assigned chromophores over wavelengths of 380-682 and retention time range of 8-15 minutes across three different samples: untreated BBOA (top panel), WS BBOA aged (middle), and Total BBOA aged (bottom). Chromophore identities were found using MZmine to identify m/z values at expected retention times, which were found using Xcalibur in Qual browser, and were verified with single ion chromatograms viewed in freestyle. Predator formula calculator was used to find

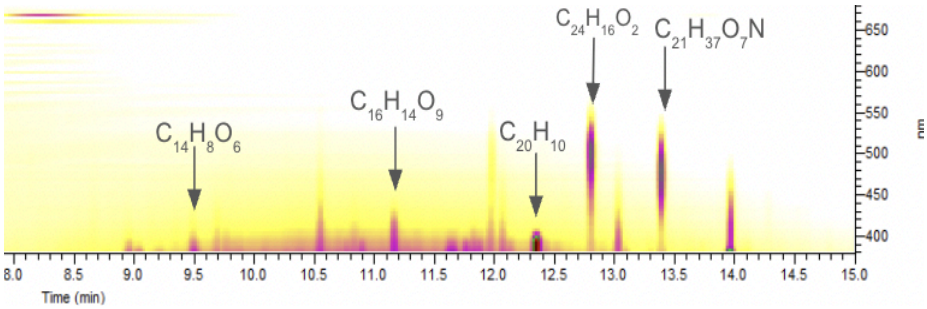

chemical formulas corresponding to the proposed m/z values found in freestyle. Formula assignments are speculative, while m/z values are confident.

Figure 8c: Total BBOA Aged

Table 1: Assigned Chromophores with Corresponding m/z Values; tentative formula assignments, m/z values are confirmed by SICs, but structural attribution remains speculative.

m/z Value	Proposed MF Assignment	Confidence
177.056 (ESI-)	$C_{10}H_{10}O_3$	Coniferyl aldehyde; very confident.
271.0271 (ESI-)	$C_{14}H_8O_6$	Likely tetrahydroxyanthraquinone; high DBE value consistent with chromophores.
351.0713 (ESI+)	$C_{16}H_{14}O_9$	Confident but speculative due to other possible, though less probable, matches.
251.0876 (ESI+)	$C_{20}H_{10}$	Speculative; likely insoluble in extracting solution.
337.122 (ESI+)	$C_{24}H_{16}O_2$	Polyaromatic compound; confident potential match.
414.2499 (ESI-)	$C_{21}H_{37}O_7N$	Highly speculative due to low DBE value.

Together, these results demonstrate that sulfuric acid catalysis efficiently transforms BBOA into more conjugated, oxygenated, nitrogen- and sulfur-containing species with enhanced light absorption. Extraction methodology further modulates the molecular fingerprints of BrC formation, contributing to the balance between absorption-driven warming and scattering-driven cooling.

6. DISCUSSION

6.1 Untreated BBOA. Unaged BBOA exhibited what is expected for untreated, resin-free BBOA as UV/Vis experiments showed a smooth UV tail with relatively weak absorption into the visible. Moreover, mass spec analysis revealed formulas dominated by CHO/CHNO constituents with moderate oxidation state (narrow O/C, H/C typically <~0.75). These spectral characteristics fall outside the strong "brown carbon window" (300–500 nm) where organic chromophores begin to contribute appreciable absorption (Moise et al., 2015; Laskin et al., 2015), providing a suitable baseline for detecting acid-induced changes in both optical response and molecular composition. The optical framing and wavelength dependence used here follow established definitions of BrC and its canonical UV–blue absorption behavior (Laskin et al., 2015).

6.2 Acid Treatment: Reaction Environment Controls BrC Formation. Exposure of BBOA to concentrated sulfuric acid produced rapid and reproducible increases in absorbance across 300–500 nm, with distinct enhancements near ~350–400 nm, consistent with BrC chromophores (Moise et al., 2015; Laskin et al., 2015). The effect was strongest in 16 M H_2SO_4 despite a ten-fold dilution relative to the UV/Vis control (note: this non-standardized BBOA concentration pertains only to the UV/Vis dataset; composition-resolved analyses were interpreted independently). The response in 10 M was modest by comparison. This contrast indicates that the reaction environment (low water activity and strong acidity) dominates over initial BBOA concentration in governing BrC production. Mechanistically, the composition shifts toward higher DBE at similar carbon number, growth of CHOS/CHNOS classes, and increased O/C at lower carbon number together point to acid-catalyzed functionalization coupled to condensation/dehydration. Pathways of acid catalyzed functionalization span sulfation of alcohols and epoxides (Surratt et al., 2010; Lin et al., 2011), esterification, and acetal/hemiacetal formation (Ervens & Volkamer, 2010) while condensation and dehydration pathways include carbonyl and phenolic oligomerization as well as sugar to HMF pathways with subsequent polymerization (Laskin et al., 2015; Liu et al., 2022). These routes are well documented in the literature for concentrated sulfate media, producing conjugated, low-volatility products that absorb in the UV–blue (Laskin et al., 2015). In atmospheric terms, 16 M is a reasonable analog for poorly hydrated stratospheric sulfate aerosol after major injections, whereas 10 M reflects a more hydrated UT/LS endmember; the weaker response at 10 M is consistent with reduced reactivity under higher water activity (Kremser et al., 2016).

6.3 Water-Extracted vs. Acid-Extracted Pathways: Two Environmental Scenarios. The two extraction protocols were designed to represent distinct atmospheric trajectories. Water-extracted (WS) samples simulate BBOA partitioning into aqueous droplets or hydrated aerosols before encountering stratospheric concentrated sulfate aerosol droplets; On the other hand, acid-extracted (Total) samples parallel direct uptake of BBOA into concentrated acid droplets (Kremser et al., 2016). Consistent with these scenarios, WS systems showed weaker, less structured absorption, with formula dominated by highly oxygenated CHOS classes, suggesting formation of organosulfate and carboxylic-acid-rich material. This pattern indicates that higher water activity suppresses condensation/dehydration while favoring functionalization (Ervens & Volkamer, 2010; Surratt et al., 2010); sulfation of polyols/epoxides and formation of acetals/esters can proceed, but extensive conjugation is less favored, yielding more moderately absorbing BrC and relatively greater scattering from polar, hygroscopic products (Laskin et al., 2015). By contrast, acid-extracted samples exhibited stronger UV–blue absorption with reproducible features near ~350–400 nm, clustering of high-DBE CHNO/CHNOS at low H/C, and broader distributions toward larger carbon numbers. These signatures are consistent with cross-linked, conjugated oligomers and organosulfate-bearing species that are stabilized in highly acidic media (Laskin et al., 2015). Increases in CHNO/CHNOS suggest enrichment or, more plausibly, preservation of N-containing material and acid-stabilized conjugation; as formation of nitroaromatics requires NOx/HNO_3 or imidazoles with unprotonated amines, which is not supported under the strongly acidic conditions employed here. Together, these results show that hydration state and matrix composition co-determine both the reaction pathways accessed and the products recovered, in line with prior work identifying sulfation/functionalization and oligomer growth as key acid-driven routes to BrC aging and SOA chromophore formation (Moise et al., 2015; Laskin et al., 2015).

6.4 Kinetics and Atmospheric Relevance. Time-series experiments indicate that the dominant acid-driven transformations occur rapidly, as the main spectral changes were established within 24 h, with little consistent evolution thereafter. Week-long, static exposure in 16M sulfuric acid produced

inconsistent anomalies, which were interpreted as laboratory artifacts of BBOA over-aging toward tar- or humins-like material, rather than atmospherically representative chemistry (Liu et al., 2022; Laskin et al., 2015). Because stratospheric sulfate aerosols persist for a few weeks to several months or upwards of a few years (Kremser et al., 2016), rapid establishment of BrC signatures is atmospherically relevant. Particles likely acquire their absorbing character early, with subsequent fate governed more by mixing, dilution, photolysis, and transport than by continued acid-only processing. The product classes and optical behavior observed here are consistent with the broader understanding of organic–sulfate interactions and BrC optical evolution.

7. CONCLUSIONS

This study demonstrates that BrC formation from BBOA is strongly governed by the chemical environment into which it is introduced, particularly under stratospherically relevant conditions. Acid-catalyzed reactions in concentrated sulfuric acid media, analogous to post-volcanic stratospheric sulfate aerosols, drive rapid, reproducible transformations in both molecular composition and optical properties. The emergence of UV–blue absorbing chromophores, coupled with the growth of CHOS and CHNOS classes and increased double bond equivalence, reflect acid-driven pathways including sulfation, esterification, acetal formation, and condensation. These mechanisms yield conjugated, low-volatility products that contribute significantly to BrC absorption.

Comparative analysis of water-extracted and acid-extracted samples reveals that hydration state plays a critical role in determining reaction pathways. Hydrated systems favor functionalization and organosulfate formation, while concentrated acid environments promote oligomerization and conjugation. The preservation of nitrogen-containing species and the absence of nitroaromatic formation under strongly acidic conditions further constrain reaction pathways accessible to BBOA in the stratosphere.

Time-resolved experiments confirm that BrC signatures are established rapidly, with minimal evolution beyond the initial 24-hour exposure. This kinetic behavior supports the atmospheric relevance of the observed transformations, suggesting that BBOA particles acquire their absorbing character early in their stratospheric lifetime. Subsequent changes are likely dominated by physical processes such as mixing, dilution, and photolysis rather than continued acid-only chemistry.

Together, these findings provide a mechanistic and compositional framework for understanding BrC aging in the stratosphere. They highlight the importance of acidity, hydration, and matrix composition in shaping the optical and molecular evolution of BBOA, offering new insight into the role of organic–sulfate interactions in post-volcanic aerosol chemistry and climate relevant radiative forcing.

8. ACKNOWLEDGMENTS

I wish to acknowledge and thank all members of the UCI Aerosol Photochemistry Group. I received substantial guidance and technical support from each and every member, which has been invaluable to my training. I would especially like to thank Professor Sergey Nizkorodov for his mentorship and support, which far exceeded my expectations. Dr. Nizkorodov fostered a collaborative lab environment that encouraged questions and exploration; this was instrumental in my learning of project design, data pipelines, and processing workflows. Most importantly, under his guidance, I was able to learn from my mistakes without scrutiny.

I would also like to thank Professor Vy Dong for the time I spent training with the Dong Group in preparation for my work with AirUCI. Her mentorship helped lay the foundation for my transition into aerosol chemistry.

Lastly, I wish to thank Dr. A.J. Shaka for his teachings, mentorship, and guidance throughout the honors thesis seminar and a rigorous four year chemistry degree. Dr. Shaka's infamous "tuffy" homework assignments during my first year were the first time I truly struggled. Never before had I looked at a problem and not known where to begin, or even what was being asked. Through his teachings, I came to understand that a lack of knowledge isn't a signal to raise the white flag, but rather a mark for the starting line.

Through the mentorship of Dr. Nizkorodov, Dr. Dong, and Dr. Shaka, I developed the technical skills and scientific knowledge to submit an Honors Thesis– a milestone I could not have foreseen given the challenges of ADHD and dyslexia.

9. REFERENCES

Altieri, K. E., Seitzinger, S. P., Carlton, A. G., Turpin, B. J., Klein, G. C., & Marshall, A. G. (2008). Oligomers formed through in-cloud methylglyoxal reactions: Chemical composition, properties, and mechanisms investigated by ultra-high resolution FT-ICR mass spectrometry. *Atmospheric Environment*, *42*(7), 1476-1490.

Andreae, M. O., & Rosenfeld, D. J. E. S. R. (2008). Aerosol–cloud–precipitation interactions. Part 1. The nature and sources of cloud-active aerosols. *Earth-Science Reviews*, *89*(1-2), 13-41.

Bond, T. C., Doherty, S. J., Fahey, D. W., Forster, P. M., Berntsen, T., DeAngelo, B. J., ... & Zender, C. S. (2013). Bounding the role of black carbon in the climate system: A scientific assessment. *Journal of geophysical research: Atmospheres*, *118*(11), 5380-5552

Bones, D. L., Henricksen, D. K., Mang, S. A., Gonsior, M., Bateman, A. P., Nguyen, T. B., ... & Nizkorodov, S. A. (2010). Appearance of strong absorbers and fluorophores in limonene‐O3 secondary organic aerosol due to NH4+‐mediated chemical aging over long time scales. *Journal of Geophysical Research: Atmospheres*, *115*(D5)..

Boucher, O., Randall, D., Artaxo, P., Bretherton, C., Feingold, G., Forster, P., ... & Lohmann, U. (2013). Rasch, 30 P., Satheesh, SK, Sherwood, S., Stevens, B., and Zhang, XY: Clouds and Aerosols. *Climate Change*.

Boucher, O. (2015). Atmospheric aerosols. In *Atmospheric Aerosols: Properties and Climate Impacts* (pp. 9-24). Dordrecht: Springer Netherlands.

Carey, F. A., & Sundberg, R. J. (2007). *Advanced organic chemistry: Part A: Structure and mechanisms* (5th ed.). Springer.

Chaturvedi, S., Kumar, A., Singh, V., Chakraborty, B., Kumar, R., & Min, L. (2023). Recent advancement in organic aerosol understanding: A review of their sources, formation, and health impacts. *Water, Air, & Soil Pollution*, *234*(12), 750.

Chen, H., Ge, X., & Ye, Z. (2018). Aqueous-phase secondary organic aerosol formation via reactions with organic triplet excited states—a short review. *Current Pollution Reports*, *4*(1), 8-12.

Cooke, M. E., Armstrong, N. C., Fankhauser, A. M., Chen, Y., Lei, Z., Zhang, Y., ... & Ault, A. P. (2024). Decreases in epoxide-driven secondary organic aerosol production under highly acidic conditions: the importance of acid–base equilibria. *Environmental Science & Technology*, *58*(24), 10675-10684.

Després, V., Huffman, J. A., Burrows, S. M., Hoose, C., Safatov, A., Buryak, G., ... & Jaenicke, R. (2012). Primary biological aerosol particles in the atmosphere: a review. *Tellus B: Chemical and Physical Meteorology*, *64*(1), 15598.

Ervens, B. T. B. W. R., Turpin, B. J., & Weber, R. J. (2011). Secondary organic aerosol formation in cloud droplets and aqueous particles (aqSOA): a review of laboratory, field and model studies. *Atmospheric Chemistry and Physics*, *11*(21), 11069-11102.

Ervens, B., & Volkamer, R. (2010). Glyoxal processing by aerosol multiphase chemistry: towards a kinetic modeling framework of secondary organic aerosol formation in aqueous particles. *Atmospheric Chemistry and Physics*, *10*(17), 8219-8244.

Fleming, L. T., Lin, P., Roberts, J. M., Selimovic, V., Yokelson, R., Laskin, J., ... & Nizkorodov, S. A. (2020). Molecular composition and photochemical lifetimes of brown carbon chromophores in biomass burning organic aerosol. *Atmospheric Chemistry and Physics*, *20*(2), 1105-1129.

George, I. J., & Abbatt, J. P. D. (2010). Heterogeneous oxidation of atmospheric aerosol particles by gas-phase radicals. *Nature Chemistry*, *2*(9), 713-722.

Guo, H., Xu, L., Bougiatioti, A., Cerully, K. M., Capps, S. L., Hite Jr, J. R., ... & Weber, R. J. (2015). Fine-particle water and pH in the southeastern United States. *Atmospheric Chemistry and Physics*, *15*(9), 5211-5228.

Hanson, D. R., Ravishankara, A. R., & Solomon, S. (1994). Heterogeneous reactions in sulfuric acid aerosols: A framework for model calculations. *Journal of Geophysical Research: Atmospheres*, *99*(D2), 3615-3629.

Jang, M., & Kamens, R. M. (2001). Atmospheric secondary aerosol formation by heterogeneous reactions of aldehydes in the presence of a sulfuric acid aerosol catalyst. *Environmental Science & Technology*, *35*(24), 4758-4766.

Jang, M., Czoschke, N. M., Lee, S., & Kamens, R. M. (2002). Heterogeneous atmospheric aerosol production by acid-catalyzed particle-phase reactions. *Science*, *298*(5594), 814-817.

Kokhanovsky, A. A. (2008). *Aerosol optics: light absorption and scattering by particles in the atmosphere*. Berlin, Heidelberg: Springer Berlin Heidelberg.

Kremser, S., Thomason, L. W., von Hobe, M., Hermann, M., Deshler, T., Timmreck, C., Toohey, M., Stenke, A., Schwarz, J. P., & Weigel, R. (2016). Stratospheric aerosol—Observations, processes, and impact on climate. *Reviews of Geophysics*, *54*(2), 278–335.

Kroll, J. H., Donahue, N. M., Jimenez, J. L., Kessler, S. H., Canagaratna, M. R., Wilson, K. R., ... & Worsnop, D. R. (2011). Carbon oxidation state as a metric for describing the chemistry of atmospheric organic aerosol. *Nature chemistry*, *3*(2), 133-139.

Laskin, A., Laskin, J., & Nizkorodov, S. A. (2015). Chemistry of atmospheric brown carbon. *Chemical reviews*, *115*(10), 4335-4382.

Lelieveld, J., Evans, J. S., Fnais, M., Giannadaki, D., & Pozzer, A. (2015). The contribution of outdoor air pollution sources to premature mortality on a global scale. *Nature*, *525*(7569), 367-371.

Li, Y., Dykema, J., Deshler, T., & Keutsch, F. (2021). Composition dependence of stratospheric aerosol shortwave radiative forcing in northern midlatitudes. *Geophysical Research Letters*, *48*(24), e2021GL094427.

Lin, P., & Yu, J. Z. (2011). Generation of reactive oxygen species mediated by humic-like substances in atmospheric aerosols. *Environmental science & technology*, *45*(24), 10362-10368.

Lin, Y. H., Zhang, Z., Docherty, K. S., Zhang, H., Budisulistiorini, S. H., Rubitschun, C. L., ... & Surratt, J. D. (2012). Isoprene epoxydiols as precursors to secondary organic aerosol formation: acid-catalyzed reactive uptake studies with authentic compounds. *Environmental science & technology*, *46*(1), 250-258.

Liu, Y., Jia, R., Dai, T., Xie, Y., & Shi, G. (2014). A review of aerosol optical properties and radiative effects. *Journal of Meteorological Research*, *28*(6), 1003-1028.

Liu, S., Zhu, Y., Liao, Y., Wang, H., Liu, Q., Ma, L., & Wang, C. (2022). Advances in understanding the humins: Formation, prevention and application. *Applications in Energy and Combustion Science*, *10*, 100062.

Masson-Delmotte, V., Zhai, P., Pirani, A., Connors, S. L., Péan, C., Berger, S., ... & Zhou, B. (2021). Climate change 2021: the physical science basis. *Contribution of working group I to the sixth assessment report of the intergovernmental panel on climate change*, *2*(1), 2391.

McNeill, V. F. (2015). Aqueous organic chemistry in the atmosphere: Sources and chemical processing of organic aerosols.

Millán, L., et al. (2022). Tonga eruption blasted unprecedented amount of water into stratosphere. *Geophysical Research Letters*. NASA Jet Propulsion Laboratory. (accessed 09/10/25) https://www.jpl.nasa.gov/news/tonga-eruption-blasted-unprecedented-amount-of-water-into-stratosphere

Moise, T., Flores, J. M., & Rudich, Y. (2015). Optical properties of secondary organic aerosols and their changes by chemical processes. *Chemical reviews*, *115*(10), 4400-4439.

National Aeronautics and Space Administration. (2021, August 17). Studying Earth's stratospheric water vapor. (accessed 09/10/25) https://www.nasa.gov/centers-and-facilities/langley/studying-earths-stratospheric-water-vapor/

Nguyen, T. K. V., Petters, M. D., Suda, S. R., Guo, H., Weber, R. J., & Carlton, A. G. (2014). Trends in particle-phase liquid water during the Southern Oxidant and Aerosol Study. *Atmospheric Chemistry and Physics*, *14*(20), 10911-10930.

Niu, X., Huang, Y., Lee, S. C., Sun, J., & Ho, K. F. (2020). Surface characterization of secondary organic aerosols from ozonolysis of monoterpene and the effects of acute lung injury in mice. *Aerosol and Air Quality Research*, *20*(7), 1675-1685.

O'Dowd, C. D., & De Leeuw, G. (2007). Marine aerosol production: a review of the current knowledge. *Philosophical Transactions of the Royal Society A: Mathematical, Physical and Engineering Sciences*, *365*(1856), 1753-1774.

Pöschl, U. (2005). Atmospheric aerosols: composition, transformation, climate and health effects. *Angewandte Chemie International Edition*, *44*(46), 7520-7540.

Pye, H. O., Nenes, A., Alexander, B., Ault, A. P., Barth, M. C., Clegg, S. L., ... & Zuend, A. (2020). The acidity of atmospheric particles and clouds. *Atmospheric chemistry and physics*, *20*(8), 4809-4888.

Ramaswamy, V., Chanin, M. L., Angell, J., Barnett, J., Gaffen, D., Gelman, M., ... & Lin, J. J. (1999). Stratospheric temperature changes: Observations and model simulations.

Robock, A. (2000). Volcanic eruptions and climate. *Reviews of geophysics*, *38*(2), 191-219.

Roy, P., Rauber, R. M., & Di Girolamo, L. (2023). A closer look at the evolution of supercooled cloud droplet temperature and lifetime in different environmental conditions with implications for ice nucleation in the evaporating regions of clouds. *Journal of the Atmospheric Sciences*, *80*(10), 2481-2501.

Schulz, M., de Leeuw, G., & Balkanski, Y. (2004). Sea-salt aerosol source functions and emissions. In *Emissions of Atmospheric Trace Compounds* (pp. 333-359). Dordrecht: Springer Netherlands.

Schum, S. K., Brown, L. E., & Mazzoleni, L. R. (2020). MFAssignR: Molecular formula assignment software for ultrahigh resolution mass spectrometry analysis of environmental complex mixtures. *Environmental Research*, *191*, 110114.

Seinfeld, J. H., & Pandis, S. N. (2016). *Atmospheric chemistry and physics: from air pollution to climate change*. John Wiley & Sons.

Sicard, M., Baron, A. A., Ranaivombola, M., Gantois, D., Millet, T., Sellitto, P., ... & Duflot, V. (2023). Radiative impact of the Hunga Tonga-Hunga Ha'apai stratospheric volcanic plume: role of aerosols and water vapor in the southern tropical Indian Ocean. *Authorea Preprints*.

Soden, B. J., Wetherald, R. T., Stenchikov, G. L., & Robock, A. (2002). Global cooling after the eruption of Mount Pinatubo: A test of climate feedback by water vapor. *science*, *296*(5568), 727-730.

Solomon, S., Rosenlof, K. H., Portmann, R. W., Daniel, J. S., Davis, S. M., Sanford, T. J., & Plattner, G. K. (2010). Contributions of stratospheric water vapor to decadal changes in the rate of global warming. *science*, *327*(5970), 1219-1223.

Squizzato, S., Masiol, M., Brunelli, A., Pistollato, S., Tarabotti, E., Rampazzo, G., & Pavoni, B. (2012). Factors determining the formation of secondary inorganic aerosol: a case study in the Po Valley (Italy). *Atmos. Chem. Phys. Discuss*, *12*, 16377-16406.

Surratt, J. D., Gómez-González, Y., Chan, A. W., Vermeylen, R., Shahgholi, M., Kleindienst, T. E., ... & Seinfeld, J. H. (2008). Organosulfate formation in biogenic secondary organic aerosol. *The Journal of Physical Chemistry A*, *112*(36), 8345-8378.

Surratt, J. D., Chan, A. W., Eddingsaas, N. C., Chan, M., Loza, C. L., Kwan, A. J., ... & Seinfeld, J. H. (2010). Reactive intermediates revealed in secondary organic aerosol formation from isoprene. *Proceedings of the National Academy of Sciences*, *107*(15), 6640-6645.

Teri, M., Gasteiger, J., Heimerl, K., Dollner, M., Schöberl, M., Seibert, P., ... & Weinzierl, B. (2025). Pollution affects Arabian and Saharan dust optical properties in the eastern Mediterranean. *Atmospheric Chemistry and Physics*, *25*(13), 6633-6662.

Tolocka, M. P., Jang, M., Ginter, J. M., Cox, F. J., Kamens, R. M., & Johnston, M. V. (2004). Formation of oligomers in secondary organic aerosol. *Environmental Science & Technology*, *38*(5), 1428-1434.

Velasco Calderón, J. C., Arora, J. S., & Mushrif, S. H. (2022). Mechanistic investigation into the formation of humins in acid-catalyzed biomass reactions. *ACS omega*, *7*(49), 44786-44795.

Xin, K., Chen, J., & Soyol-Erdene, T. (2023). Formation mechanism and source apportionment of nitrate in atmospheric aerosols. *APN Science Bulletin*, *13*(1), 102-111.

Zhang, Z., Xu, W., Lambe, A. T., Hu, W., Liu, T., & Sun, Y. (2024). Insights Into Formation and Aging of Secondary Organic Aerosol From Oxidation Flow Reactors: A Review. *Current Pollution Reports*, *10*(3), 387-400.

Zhu, Y., Bardeen, C. G., Tilmes, S., Mills, M. J., Wang, X., Harvey, V. L., ... & Toon, O. B. (2022). Perturbations in stratospheric aerosol evolution due to the water-rich plume of the 2022 Hunga-Tonga eruption. *Communications Earth & Environment*, *3*(1), 248.